Journal of Robotics and Control (JRC)
Volume 5, Issue 4, 2024
ISSN: 2715-5072, DOI: 10.18196/jrc.v5i4.22139

Investigation of Optimal Controllers on Dynamics Performance of Nonlinear Active Suspension Systems with Actuator Saturation

Mohammed A. Al-Ali [1*], Omar F. Lutfy [2], Huthaifa Al-Khazraj [3]
[1, 2, 3] Control and Systems Engineering Department, University of Technology-Iraq, Baghdad 10066, Iraq
Email: [1] cse.22.19@grad.uotechnology.edu.iq, [2] 60156@uotechnology.edu.iq, [3] 60141@uotechnology.edu.iq,
*Corresponding Author

Abstract—**This study investigates designing optimal controllers on the dynamics performance of active suspension systems. The study incorporates nonlinearities and actuator saturation in the mathematical model of the suspension system for more reasonable representation of the real system. To improve ride comfort and stability performance in the presence of road disturbances, this study proposes two control frameworks including the Proportional-Integral-Derivative (PID) controller and the State Feedback (SF) controller. The focus of the study is to overcome the limitations of existing approaches in handling the actuator saturation in the controller design. To attain a better performance of the two proposed controllers including the input control constraint, a Grey Wolf Optimization (GWO) has been introduced to improve the searching process for the optimal values of the controllers' adjustable parameters. The simulation results using MATLAB show that the proposed controllers exhibit a good performance in normal operation and in a robustness test involving system parameters' changes. In terms of improving the response of the system, the GWO-PID controller shows a better response than that of the GWO-SF controller. Based on the Integral Square Error (ISE) index, the ISE is reduced by 16.67% using the GWO-PID controller compared to the GWO-SF controller.**

Keywords—Active Suspension System; Nonlinear Control; Optimal Control; PID Controller; State Feedback Controller; Grey Wolf Optimization.

I. Introduction

One of the most essential components of a car is the suspension system, which is used to reduce the impact of road disturbance in order to provide a comfort ride and stability performance. The suspension system connects a car to its wheels through a network of springs, shock absorbers, and linkages. A mechanism that physically separates the vehicle's body from its wheels is known as the suspension system. Road comfort is directly improved by the suspension system of the vehicle by minimizing the vertical acceleration transmitted to the passenger [1]-[3]. Over the past few decades, a significant amount of study has focused on the examination of a variety of suspension system types, such as passive, semiactive, and active suspension systems [4]. In particular, a basic passive suspension system consists of a spring that works as an energy storing element and a damper that works as an energy dissipating element [5]. Unlike the passive suspension system, the semiactive type employs an adjustable damper to reduce the suspension vibration after the presence of road disturbances [6]. In contrast to the previous two types, the active suspension system has a hydraulic actuator that allows the suspension force to be adjusted based on the vehicle's road condition [7].

The utilization of feedback control has been proven over the years as a good mechanism that could be used to improve the performance of the control system [8]. In this regard, various attempts have been made to apply different feedback controller frameworks for suspension systems to achieve a better ride comfort. In the context of linear models, Sam et al. [9] proposed a robust strategy based on Proportional-Integral Sliding Mode Control (PI-SMC). A quarter-car model is used in the study. The mathematical model of the suspension system is presented in a state space formulation. The results of the PI-SMC controller show a better performance compared to the Linear Quadratic Regulator (LQR) method and the passive suspension system. Another application of SMC into the suspension system was implemented by [2] and [4]. Zhou [2] developed an optimal SMC to improve the dynamic quality of SMC control for an active suspension system. Genetic Algorithm (GA) is introduced to tune the weight coefficients of the SMC's control law. The simulation results show that the optimal SMC based on GA controller has better control performance than the traditional SMC controller. Zhang [4] presented a feed-forward and feedback SMC for active suspension systems based on quarter-car model. Based on reading some state variables of the suspension system, an analytic term and a disturbances compensation term are developed to improve the performance of the SMC. The result of a numerical example is shown that proposed feed-forward and feedback SMC has a better effect to attenuate the random road surface disturbances than traditional SMC controller. In addition, Salem and Aly [10] presented a comparative study between the PID controller and a Fuzzy Logic Controller (FLC) to control an active suspension system. The outcomes showed that the FLC provides good results compared to those of the PID controller. Moreover, Romsai et al. [11] proposed an optimized approach for the classical PID controller based on Lévy-flight intensified current search optimization approach.

Recently, Al-Khazraji [3] presented a Proportional-Derivative State Feedback (PDSF) controller approach. Two meta-heuristic optimizations named Bees Algorithm (BA) and Grey Wolf Optimization (GWO) are proposed to optimize the feedback gain matrix of the PDSF controller based on the Integral Time of Absolute Error (ITAE) index. The results show the superiority of the BA-based PDSF controller in terms of reducing the ITAE index in comparison with the results obtained from GWO based PDSF. Abut and Salkim [12] presented a comparative study between Linear Quadratic Regulator (LQR), FLC, and fuzzy-LQR control algorithms to the suspension system for active control. It was found that the car's ride comfort has been significantly improved by the fuzzy-LQR control method. An LQR control strategy utilizing Ant Colony Optimization (ACO) in the active suspension system was presented by Manna et al. [13]. They used it in an experimental setting on a quarter-car model. In three track profiles, the suggested approach was experimentally contrasted with the traditional LQR and Model Predictive Control (MPC) approaches. In comparison to the classically tuned LQR and MPC, the results demonstrated that the proposed method significantly reduced the acceleration of the body due to uneven road profiles. It has also been demonstrated to greatly enhance vehicle handling and passenger comfort.

For more reasonable representation of the real system, many papers have considered the nonlinearity in the modeling of the suspension system. In this direction, Aldair et al. [14] presented an optimized Fractional Order PID (FOPID) controller for a nonlinear active suspension system. Sadeghi et al. [15] developed a nonlinear PD controller approach for a nonlinear quarter car suspension system. The proposed controller is compared with the results of a fuzzy-PID controller show that the proposed controller is more stable and has less damping in response while the system speed is improved. In another work, Nagarkar et al. [16] compared the performance of the PID controller and that of the LQR controller in controlling the nonlinear suspension system. Sun et al. [17] proposed an adaptive backstepping control scheme for nonlinear suspension systems to improve ride comfort in the presence of parametric uncertainties. However, the main limitation of the above-mentioned works is that they did not consider the actuator saturation. For real implementation of the proposed controller, the actuator saturation has to be considered as a physical limit of the output of the actuator.

To address the problem of road disturbance in order to provide a comfort ride and stability performance using a nonlinear model of the suspension system considering the actuator saturation, this study proposes and compares the performance of two control frameworks including the PID controller and the SF controller. In this context, determining the two controllers' design variables to generate control signals that make the nonlinear system follow a desired performance is a very challenging task. In particular, many authors choose to utilize metaheuristic optimization methods to find the best controller adjustable parameters since they are more effective than using the trial-and-error method [18]-[20]. The metaheuristic algorithms have been successfully applied to solve a wide range of optimization-related problems [21]-[24]. To address the tuning problem in this work, the Grey Wolf Optimization (GWO) has been employed. GWO has a substantial growth in diverse domains due to its impressive features over others, such as it can be easily adapted, parameter-free, derivative-free, and computational-less [25].

Researchers have been used the GWO in the tuning process in numerous application. For example, Sule et al. [26] optimized the Proportional Integral (PI) controller for fixed-speed wind turbine using GWO. Verma et al. [27] adopted the GWO to find the optimal value of the FOPID controller for two classes of systems including time-delay and higher-order system. Dogruer [28] optimized a cascaded proportional-integral plus proportional-derivative (PI-PD) controller for unstable system based on GWO. Then, Hasan et al [29] optimized the fractional order PI-PD (FOPI-FOPD) controller design for rotary inverted pendulum based on GWO. In terms of SF controller, Sun et al. [30] presented an optimal SF controller approach for a permanent-magnet synchronous hub motor (PMSHM) drive using GWO. Jasim [31] optimized the SF controller for two-wheeled self-balancing robot based on GWO.

To end this, this research contributes to the existing body of knowledge as follows:

- Investigating the performance of the PID and the SF controllers for nonlinear model of the active suspension systems to address the problem of road disturbance in order to provide a comfort ride and stability performance.
- The paper considers the actuator saturation in addition to the uncertainties in the car body mass to represent the physical systems in reality.
- To enhance the performance of the PID and the SF controllers, GWO is introduced instead of try-and-error method for finding the optimal value of controllers' adjustable parameters.

The rest of this paper is organized as follows: Section 2 gives the mathematical model of the nonlinear active suspension system. In Section 3, the PID and SF controllers have been explained. Section 4 presents the GWO. The validation of the proposed optimized controllers is reported in the Section 5 and finally, the conclusion is summarized in Section 6.

II. SYSTEM MODELING

First, the mathematical model of the active suspension system is given in this section. The active suspension system can be represented by the 2DOF Mass-Spring-Damper (MSD) system, as illustrated in Fig. 1 [9] in which m_b and m_w are the masses of the car body and the wheel, respectively, F_s, F_d, F_a and F_t are the forces that are generated by the wheel spring, the wheel damper, the actuator, and the spring of the tire, respectively, d is the road disturbance, x_1 and x_2 are the positions of the car body and the wheel, respectively, x_3 and x_4 are the velocities of the car body and the wheel, respectively, and $\dot{x}_3$ and $\dot{x}_4$ are the acceleration variables of the car body and the wheel, respectively.

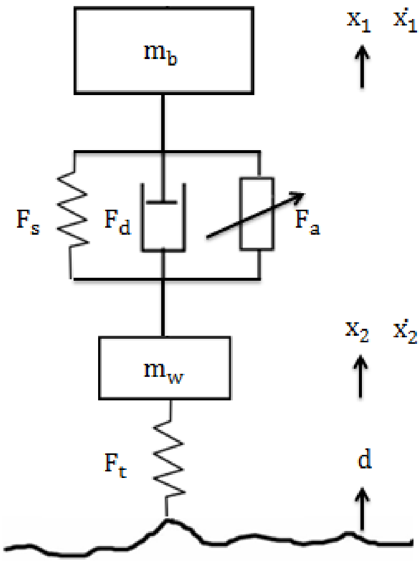

Fig. 1. Active suspension system

Based on the Newten's law, the motion equation for the masses of the car body and the wheel are given by [11]:

$$m_b\dot{x}_3 = -F_s - F_d + F_a \tag{1}$$

$$m_w\dot{x}_4 = F_s + F_d - F_a - F_t \tag{2}$$

The nonlinear force (F_s) is computed as follows [16][32]:

$$F_s = k_{sl}(x_1 - x_2) + k_{sn}(x_1 - x_2)^3 \tag{3}$$

The nonlinear force (F_d) is computed as follows [33]:

$$F_d = c_{dl}(\dot{x}_1 - \dot{x}_2) + c_{sn}(\dot{x}_1 - \dot{x}_2)^2 \tag{4}$$

The force (F_t) is computed as follows [16] [33]:

$$F_t = k_t(x_2 - d) \tag{5}$$

where $k_{sl}, k_{sn}, c_{dl}, c_{sn},$ and k_t are the linear stiffness coefficient of the spring, the nonlinear stiffness coefficient of the spring, the linear damper coefficient of the spring, the nonlinear damper coefficient of the spring, and the stiffness coefficient of the spring in the tire.

By substituting Eq. (3) and Eq. (4) into Eq. (1) and Eq. (2), we obtain:

$$\begin{aligned} m_b\dot{x}_3 = -(k_{sl}(x_1 - x_2) + k_{sn}(x_1 - x_2)^3) \\ - (c_{dl}(\dot{x}_1 - \dot{x}_2) + c_{sn}(\dot{x}_1 - \dot{x}_2)^2) \\ + F_a \end{aligned} \tag{6}$$

$$\begin{aligned} m_w\dot{x}_4 = (k_{sl}(x_1 - x_2) + k_{sn}(x_1 - x_2)^3) \\ + (c_{dl}(\dot{x}_1 - \dot{x}_2) + c_{sn}(\dot{x}_1 - \dot{x}_2)^2) \\ - F_a - (k_t(x_2 - d)) \end{aligned} \tag{7}$$

For the purpose of the control design, the state variable equations of the nonlinear suspension system are defined as:

$$\dot{x}_1 = x_3 \tag{8}$$

$$\dot{x}_2 = x_4 \tag{9}$$

$$\begin{aligned} \dot{x}_3 = \frac{1}{m_b}((-(k_{sl}(x_1 - x_2) + k_{sn}(x_1 - x_2)^3) \\ - (c_{dl}(\dot{x}_1 - \dot{x}_2) \\ + c_{sn}(\dot{x}_1 - \dot{x}_2)^2) + F_a)) \end{aligned} \tag{10}$$

$$\begin{aligned} \dot{x}_4 = \frac{1}{m_w}\Big((k_{sl}(x_1 - x_2) + k_{sn}(x_1 - x_2)^3) \\ + (c_{dl}(\dot{x}_1 - \dot{x}_2) \\ + c_{sn}(\dot{x}_1 - \dot{x}_2)^2) - F_a \\ - (k_t(x_2 - d))\Big) \end{aligned} \tag{11}$$

III. CONTROLLER DESIGN

In this section, the details and the procedure of designing the PID controller and the SF controller for the nonlinear suspension system are presented. These controllers designed for the suspension system aim to increase car handling and passenger comfort by reducing the vibrations that occur in passive suspension systems. Specifically, the PID and the SF controllers are frequently engaged in controlling linear systems, where the PID controller design parameters can be found using the classical techniques, such as Ziegler-Nichols method for the PID controller and the pole placement method for the SF controller. However, to utilize these controllers for nonlinear systems, the system is required to be linearized around an operation point. However, this approach could be practically applied for systems that have a small region of operation [34]. To overcome this restriction, in this paper, the swarm optimization is proposed to handle the tuning process of the PID and the SF controllers' design variables for the nonlinear suspension system.

A. The PID Controller

The PID controllers have been successfully implemented in various control design problems [35]-[36]. The objective of the PID controller design is to manipulate the dynamic of the system to maintain the system in a stable state and/or reach a desired state [37].

Particularly, the control action (u) of the PID controller results from the summation of three terms, as shown in Fig. 2. After measuring the output (y) of the process, the error (e) is determined by subtracting the reference (i.e. the desired output) (y_r) from the measured output (y). Then, the proportional term adjusts u based on the weighted gain K_p of e of the process. Moreover, the integral term adjusts u based on the weighted gain K_i of the integration of the process error. Finally, the derivative term adjusts u based on the weighted gain K_d of the rate of change of the process error. The final control law of the PID controller is defined as follows [38][39]:

$$u = K_p e + K_i \int_0^t e\,dt + K_d\frac{de}{dt} \tag{12}$$

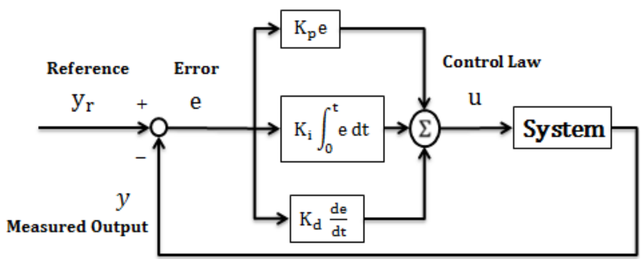

Fig. 2. The System with the PID controller

B. State Feedback Controller

The SF controller is a promising approach to design a controller, provided that the states of the system are measurable and that the system is controllable [40]. The SF controller is depicted in Fig. 3.

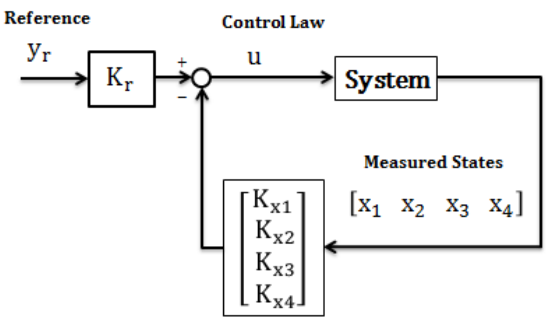

Fig. 3. The system with the SF controller

The SF controller shapes the response of the system by adjusting the system poles' location towards the desired location. More precisely, the control action u of the SF controller is computed based on the error between the weighted gain K_r of the desired output y_r and the weighted gains K_x of the system states, as given below [34]:

$$u(t) = K_r\, y_r - \begin{bmatrix} K_{x1} \\ K_{x2} \\ K_{x3} \\ K_{x4} \end{bmatrix} [x_1 \quad x_2 \quad x_3 \quad x_4] \tag{13}$$

IV. Grey Wolf Optimization

In this work, the tuning process of the PID and the SF controllers is formulated as an optimization problem, as opposed to the case of using the trial-and-error method, which is a time-consuming method. Subsequently, the optimization problem is solved by applying the Grey Wolf Optimization (GWO) technique.

The GWO is a meta-heuristic optimization technique introduced by Mirjalili et al. [41] in 2014 motivated by the social predatory behaviour of the grey wolves. According to Mirjalili et al. work, the grey wolves were divided into four levels. Alpha wolves (α) are the first level, which is in charge of leading the wolves and making decisions. The second level consists of the beta wolves (β) that are less experienced than the alpha wolves and serve as the alphas' advisors. The delta wolves (δ) belong to the third level, and they provide betas and alphas with information. Lastly, the remaining wolves are named the omega wolves (ω) [42]. The hierarchy of GWO's is shown in Fig. 4.

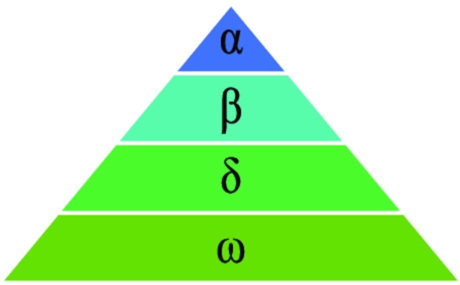

Fig. 4. Hierarchy of GWO's

The leaders (alphas) are a male and a female. They are mostly responsible for making decisions about hunting, sleeping place, time to wake, and so on. The alpha's decisions are dictated to the pack [43]. However, some kind of democratic behaviour has also been observed, in which an alpha follows the other wolves in the pack. In gatherings, the entire pack acknowledges the alpha by holding their tails down. The alpha wolf is also called the dominant wolf since his/her orders should be followed by the pack. The alpha wolves are only allowed to mate in the pack. Interestingly, the alpha is not necessarily the strongest member of the pack but the best in terms of managing the pack. This shows that the organization and discipline of a pack is much more important than its strength [44].

The second level in the hierarchy of grey wolves is beta. The betas are subordinate wolves that help the alpha in decision-making or other pack activities [45]. The beta wolf can be either male or female, and he/she is probably the best candidate to be the alpha in case one of the alpha wolves passes away or becomes very old. The beta wolf should respect the alpha, but commands the other lower-level wolves as well. It plays the role of an advisor to the alpha and discipliner for the pack. The beta reinforces the alpha's commands throughout the pack and gives feedback to the alpha [46].

The lowest ranking grey wolf is omega. The omega plays the role of scapegoat. Omega wolves always have to submit to all the other dominant wolves [47]. They are the last wolves that are allowed to eat. It may seem the omega is not an important individual in the pack, but it has been observed that the whole pack face internal fighting and problems in case of losing the omega [48]. This is due to the venting of violence and frustration of all wolves by the omega(s). This assists satisfying the entire pack and maintaining the dominance structure. In some cases, the omega is also the babysitters in the pack [49]. If a wolf is not an alpha, beta, or omega, he/she is called subordinate (or delta in some references). Delta wolves have to submit to alphas and betas, but they dominate the omega [50].

The Pseudo code of the GWO algorithm is given in Fig 5. The hunting task in GWO involves three processes, including searching for a prey, encircling the prey, and attacking the prey. More specifically, the process of moving the wolf towards the prey is mathematically formulated as follows [51]:

$$C_{wo} = 2r \tag{14}$$

$$A_{wo} = (2a_{wo}r) - a \tag{15}$$

$$D_{wo} = \left|\left(C_{wo}W_{wop}(itr)\right) - W_{wo}(itr)\right| \tag{16}$$

$$W_{wo}(itr+1) = W_{wop}(itr) - (A_{wo}D_{wo}) \tag{17}$$

where $C_{wo}, A_{wo},$ and D_{wo} are coefficients used by the GWO to determine the update position of each wolf. W_{wop} is the position of the wolf. $r, a_{wo},$ and itr represent a random value generated between [0, 1], a coefficient determined by the user, and the iterations index, respectively.

Based on the GWO concept, the three wolves. (α, β and δ) serve as a guide for the wolves during the hunting process.

1. Input

- Objective function, Population size (N), Number of iteration (T_{max}), coefficient value a

2. Initialization

- Initialize population N
- Evaluate objective function

3. Loop:

- while (itr < T_{max})
  - Find $W_{wo\alpha}, W_{wo\beta}$ *and* $W_{wo\delta}$
  - For each wolf:
    - ✓ Calculate C_{wo} as in Eq. (14) and A_{wo} as in Eq. (15)
    - ✓ Update the information of alphas α based on Eq. (18) and (19)
    - ✓ Update the information of betas β based on Eq. (20) and (21)
    - ✓ Update the information of deltas δ based on Eq. (22) and (23)
    - ✓ Update wolf 's position based on Eq. (24)
  - Evaluate the objective function
  - Perform greedy selection and update the optimal solution
  - itr = itr + 1
- end while

4. Print the Optimal Solution

Fig. 5. The GWO's pseudo code

As a result, each of these three wolf groups should supply the best information that makes other wolves change their movement. Thus, they are represented by the following equations [52]:

The information of the α wolf is given by:

$$D_{wo\alpha} = |(C_{wo1}W_{wo\alpha}) - W_{wo}(itr)| \tag{18}$$

$$W_{wo1} = W_{wo\alpha} - (A_{wo1}D_{wo\alpha}) \tag{19}$$

The information of the β wolf is given by:

$$D_{wo\beta} = |(C_{wo2}W_{wo\beta}) - W_{wo}(itr)| \tag{20}$$

$$W_{wo2} = W_{wo\beta} - (A_{wo2}D_{wo\beta}) \tag{21}$$

The information of the δ wolf is given by:

$$D_{wo\delta} = |(C_{wo3}W_{wo\delta}) - W_{wo}(itr)| \tag{22}$$

$$W_{wo3} = W_{wo\delta} - (A_{wo3}D_{wo\delta}) \tag{23}$$

After the best information of the three wolves (W_{wo1}, W_{wo2} and W_{wo3}) is collected, the new position of the individual wolf is given by:

$$W_{wo}(itr+1) = \frac{W_{wo1} + W_{wo2} + W_{wo3}}{3} \tag{24}$$

V. COMPUTER SIMULATION RESULTS

In this section, the simulation results of the PID and the SF controllers to control the nonlinear suspension system utilizing MATLAB are presented. The system's parameters are provided in Table I [33]. The two controller configurations PID and SF controllers based GWO optimization are shown in Fig. 6 and Fig. 7. The profile of the road disturbance consists of two bumps for a 5-second period of time, which is selected as follows [3]:

$$d = \begin{cases} \gamma_1(1 - cos(4\pi t_{sim})), & 0 \le t_{sim} \le 0.5 \\ \gamma_2(1 - cos(4\pi t_{sim})), & 2 \le t_{sim} \le 2.5 \\ 0, & otherwise \end{cases} \tag{25}$$

where the parameters γ_1 and γ_2 are used to shape the bumps, and they are selected to be 0.02 and 0.03, respectively, representing two bumps with heights of 0.04m and 0.06m, respectively.

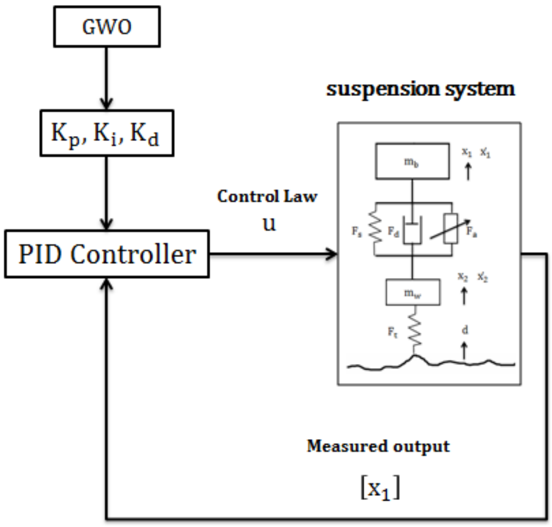

Fig. 6. Proposed PID controller tuned by GWO

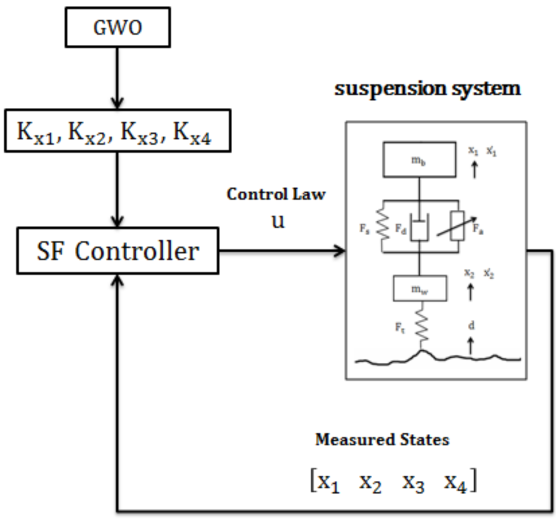

Fig. 7. Proposed SF controller tuned by GWO

Eq. (8)-(11) are used to simulate the dynamics of the suspension system. The Integral Square Error (ISE) criterion was selected as a cost function for the GWO to improve the performance of the PID and the SF controllers. This ISE index is given by [11]:

$$ISE = \int_0^{t_{sim}} e^2 \, dt \tag{26}$$

where t_{sim} denotes the simulation time and e is the output deviation, representing the error between the position of the body mass x_1 and the desired trajectory.

TABLE I. QUARTER CAR ACTIVE SUSPENSION SYSTEM PARAMETERS

Parameters	Value
Body mass (m_b)	500 Kg
Wheel mass (m_w)	40 Kg
Linear stiffness of the spring (k_{sl})	16021 N/m
Nonlinear stiffness of the spring (k_{sn})	180000 N/m^3
Stiffness of the tire spring (k_t)	240000 N/m
Linear damping factor of the damper (c_l)	1419 Ns/m
Nonlinear damping factor of the damper (c_n)	400 Ns^2/m^2

It must be pointed out that the input force of the actuator to the suspension system is saturated by ±700 N. As a result, the tuning process of the controllers based on the GWO for the nonlinear suspension system can be formulated as an optimization problem, as follows [3]:

$$\begin{gathered} minimize\ ISE(var) \\ s.t \\ -700 \geq u \geq 700 \end{gathered} \tag{27}$$

where ISE is the objective function that needs to be minimized. The decision vectors (var) are the PID controller's gains (K_p, K_i, and K_d), as given in Eq. (12), and the SF controller's feedback gain matrix (K_{x1}, K_{x2}, K_{x3}, and K_{x4}), as given in Eq. (13). Accordingly, the saturation limit of the control input u imposes a constraint in the optimization problem. The parameters of the GWO are provided in Table II. The best setting of the GWO parameters are selected after repeating the simulation several times with different values until achieving the desired control performance. In this regard, the convergence behavior of the GWO is shown in Fig. 8.

TABLE II. GWO'S PARAMETERS

Parameter	Value
Population size (N)	25
Number of iterations (T_{max})	35
Coefficient value (a)	2

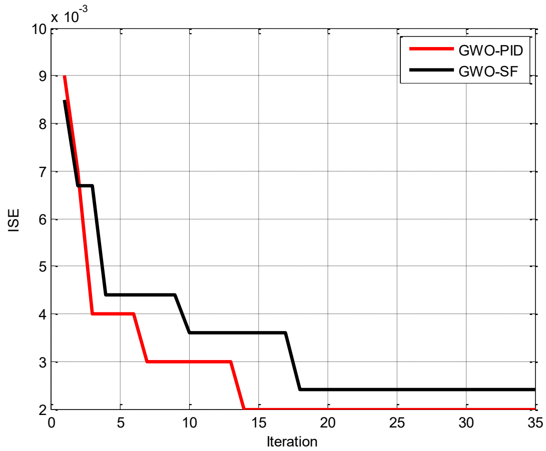

Fig. 8. GWO's convergence for the SF and the PID controllers

The values of the designed parameters for the PID and the SF controllers are given in Table III. Fig. 9 and Fig. 10 illustrate the control law and the response of the two controlled systems, respectively. The corresponding numerical value of the ISE is reported in Table IV. From Fig. 9, it can be observed that the control signals for the two controllers are within the acceptable force range of the actuator. Moreover, in Fig. 10, it can be seen that the GWO-PID controller has achieved better performance than that of the GWO-SF. This result can be validated numerically from Table IV, where it is obvious that the value of the ISE index for the GWO-PID controller (2×10^{-3}) is less than the value of the ISE index for the GWO-SF controller (2.4×10^{-3}).

TABLE III. OPTIMAL SETTING OF THE CONTROLLERS

Controller	Parameters	Values
PID Controller	K_p	11262
	K_i	20
	K_d	4990
SF Controller	K_{x_1}	5240
	K_{x_2}	1720
	K_{x_3}	3850
	K_{x_4}	400

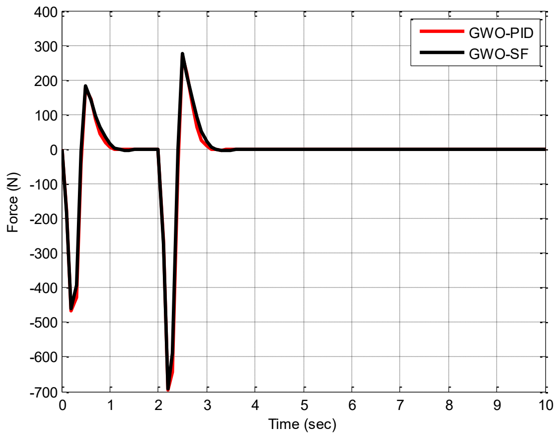

Fig. 9. Control law of the controllers

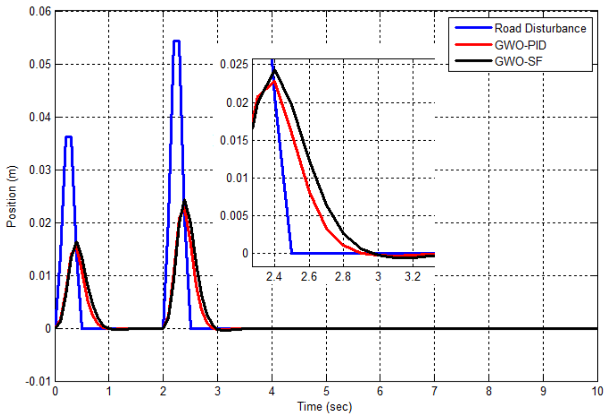

Fig. 10. Suspension system response

TABLE IV. PERFORMANCE COMPARISON

Index	GWO-PID	GWO-SF
ISE	2×10^{-3}	2.4×10^{-3}

In practical, the mass of the car body varies with the number of passengers in a car. Therefore, to evaluate the robustness of the two controllers against the uncertainty in the mass of the car body, it was assumed that the mass of the car body is changed by $\pm 20\%$ of its value. Fig. 11 and Fig. 12 show the control law and the response of the two controlled systems when the mass of the car body is increased by 20%, respectively. The corresponding numerical value of the ISE is reported in Table V. Moreover, Fig. 13 and Fig. 14 show the control law and the response of the two controlled systems when the mass of the car body is decreased by 20%, respectively. The corresponding numerical value of the ISE is reported in Table VI.

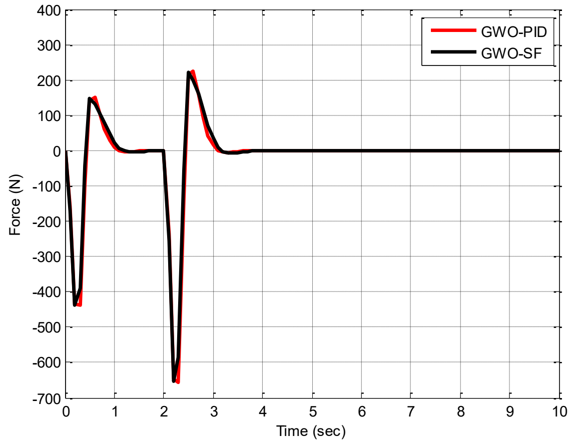

Fig. 11. Control law of the controllers when the mass of the car body increased by 20%

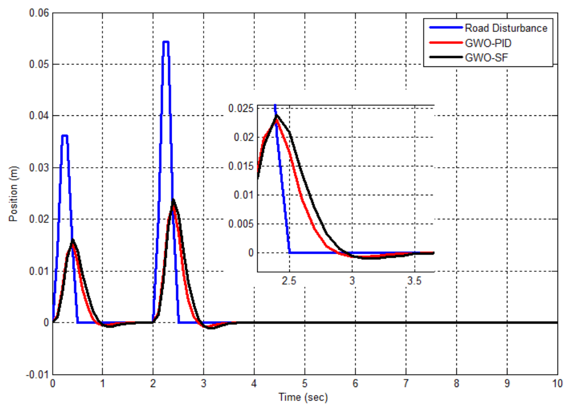

Fig. 12. Suspension system response when the mass of the car body increased by 20%

TABLE V. PERFORMANCE INDEX WHEN THE MASS OF THE CAR BODY IS INCREASED BY 20%

Index	GWO-PID	GWO-SF
ISE	2.1×10^{-3}	2.5×10^{-3}

It can be revealed based on Fig. 11 and Fig. 13 that the control signal for the two controllers with the two cases is within the acceptable force range of the actuator. Moreover, in Fig. 12 and Fig. 14, it can be seen that the GWO-PID controller has achieved better performance than that of the GWO-SF. This result can be validated numerically from Table V and Table VI. Table V illustrates that the value of the ISE index for the GWO-PID controller (2.1×10^{-3}) is less than the value of the ISE index for the GWO-SF controller (2.5×10^{-3}) in the case when the mass of the car body is increased by 20%. Table VI illustrates that the value of the ISE index for the GWO-PID controller (2×10^{-3}) is less than the value of the ISE index for the GWO-SF controller (2.4×10^{-3}) in the case when the mass of the car body is decreased by 20%.

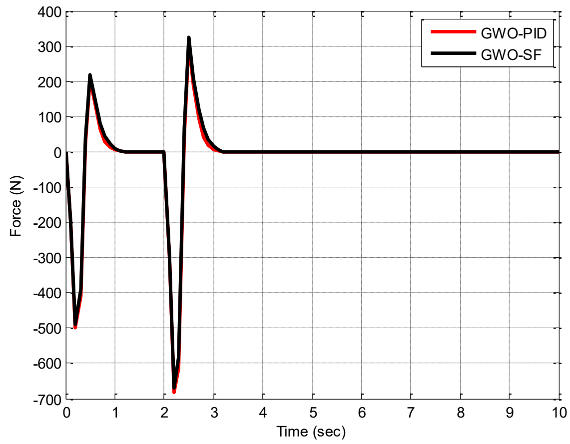

Fig. 13. Control law of the controllers when the mass of the car body decreased by 20%

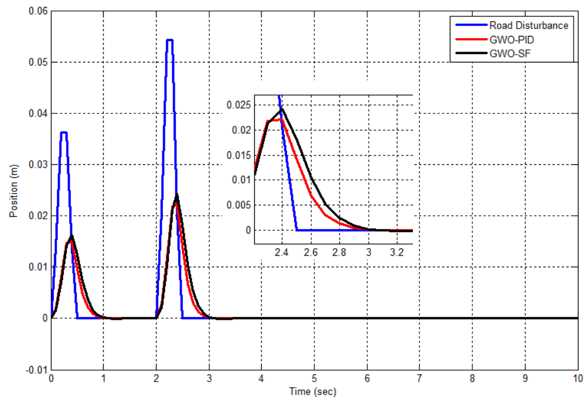

Fig. 14. Suspension system response when the mass of the car body decreased by 20%

TABLE VI. PERFORMANCE INDEX WHEN THE MASS OF THE CAR BODY IS DECREASED BY 20%

Index	GWO-PID	GWO-SF
ISE	2×10^{-3}	2.4×10^{-3}

These results sufficiently indicate that the GWO-PID controller has stronger robustness in improving vehicle body stability and ride comfort in the presence of the uncertainty in the mass of the car body.

VI. CONCLUSION

Undesirable vibrations occur in suspension systems. Within continuous changes in the business environment and market demand, an improved control system of the suspension system is an important contribution for riding comfort and the road-holding ability. In this paper, the PID controller and the SF controller were designed to act as the active controllers for the suspension system, in which the nonlinearities and actuator saturation were taken into account. The two controllers' parameters were tuned using the GWO technique based on minimizing the ISE index. The numerical simulation results using MATLAB show that the ISE of the GWO-PID controller is less than the ISE of the GWO-SF controller, which leads to improve the ride comfort. Additionally, with $\pm 20\%$ change in the mass of the car body condition, the outcomes show that the GWO-PID controller stands out by delivering superior performance and speed in the system's response.

The work can be extended in different direction as Future works. For example, nonlinear controllers [53]-[54] can be used instead of the PID and SF controllers. In terms of tuning the controllers' parameter, other optimization techniques can be used [55]. In applying the SF controller, all states were assumed to be measured. Hence, observers [56] can be applied to overcome this issue in the future.

REFERENCES

[1] K. D. Rao and S. Kumar, "Modeling and simulation of quarter car semi active suspension system using LQR controller," in *Advances in Intelligent Systems and Computing*, pp. 441–448, 2015.

[2] C. Zhou, X. Liu, W. Chen, F. Xu, and B. Cao, "Optimal sliding mode control for an active suspension system based on a genetic algorithm," *Algorithms*, vol. 11, no. 12, p. 205, 2018.

[3] H. Al-Khazraji, "Optimal design of a Proportional-Derivative State Feedback controller based on meta-heuristic optimization for a quarter car suspension system," *Math. Model. Eng. Probl*., vol. 9, no. 2, pp. 437–442, 2022.

[4] B. L. Zhang, G.-Y. Tang, and F.-L. Cao, "Optimal sliding mode control for active suspension systems," in *2009 International Conference on Networking, Sensing and Control*, pp. 351-356, 2009.

[5] M. Nagarkar and G. J. Vikhe Patil, "Optimization of the linear quadratic regulator (LQR) control quarter car suspension system using genetic algorithm," *Ing. Investig*., vol. 36, no. 1, pp. 23–30, 2016.

[6] F. Yakub, P. Muhammad, Z. H. C. Daud, A. Y. A. Fatah, and Y. Mori, "Ride comfort quality improvement for a quarter car semi-active suspension system via state-feedback controller," in *2017 11th Asian Control Conference (ASCC)*, pp. 406-411, 2017.

[7] R. Bai and D. Guo, "Sliding-mode control of the active suspension system with the dynamics of a hydraulic actuator," *Complexity*, vol. 2018, pp. 1–6, 2018.

[8] H. AL-Khazraji, C. Cole, and W. Guo, "Dynamics analysis of a production-inventory control system with two pipelines feedback," *Kybernetes*, vol. 46, no. 10, pp. 1632–1653, 2017.

[9] Y. M. Sam, J. H. S. Osman, and M. R. A. Ghani, "A class of proportional-integral sliding mode control with application to active suspension system," *Syst. Control Lett*., vol. 51, no. 3–4, pp. 217–223, 2004.

[10] M. M. Salem and A. A. Aly, "Fuzzy control of a quarter-car suspension system," *International Journal of Computer and Information Engineering*, vol. 3, no. 5, pp. 1276–1281, 2009.

[11] W. Romsai, A. Nawikavatan, and D. Puangdownreong, "Application of Lévy-flight intensified current search to optimal PID controller design for active suspension system," *International Journal of Innovative Computing, Information and Control*, vol. 17, no. 2, pp. 483–497, 2021.

[12] T. Abut and E. Salkim, "Control of quarter-car active suspension system based on optimized fuzzy linear quadratic regulator control method," *Applied Sciences*, vol. 13, no. 15, 2023.

[13] S. Manna *et al*., "Ant colony optimization tuned closed-loop optimal control intended for vehicle active suspension system," *IEEE Access*, vol. 10, pp. 53735–53745, 2022.

[14] A. A. Aldair and W. J. Wang, "Design of fractional order controller based on evolutionary algorithm for a full vehicle nonlinear active suspension systems," *International Journal of Control and Automation*, vol. 3, no. 4, pp. 33–46, 2010.

[15] M. S. Sadeghi, F. Bavafa, S. M. S. Alavi, and S. Varzandian, "Nonlinear PD controller design for a nonlinear quarter car suspension system," in *The 2nd International Conference on Control, Instrumentation and Automation*, pp. 231-235, 2011.

[16] M. P. Nagarkar, Y. J. Bhalerao, G. J. V. Patil, and R. N. Z. Patil, "Multi-objective optimization of nonlinear quarter car suspension system – PID and LQR control," *Procedia Manuf*., vol. 20, pp. 420–427, 2018.

[17] W. Sun, H. Pan, Y. Zhang, and H. Gao, "Multi-objective control for uncertain nonlinear active suspension systems," *Mechatronics (Oxf.)*, vol. 24, no. 4, pp. 318–327, 2014.

[18] H. AL-Khazraji, C. Cole, and W. Guo, "Optimization and simulation of dynamic performance of production–inventory systems with multivariable controls," *Mathematics*, vol. 9, no. 5, p. 568, 2021.

[19] N. M. Noaman, A. S. Gatea, A. J. Humaidi, S. K. Kadhim, and A. F. Hasan, "Optimal tuning of PID-controlled magnetic bearing system for tracking control of pump impeller in artificial heart," *Journal Européen des Systèmes Automatisés*, vol. 56, no. 1, 2023.

[20] A. K. Hamoudi and L. T. Rasheed, "Design and implementation of adaptive backstepping control for position control of propeller-driven pendulum system," *J. Eur. Syst. Autom*., vol. 56, no. 2, pp. 281–289, 2023.

[21] H. Al-Khazraji, S. Khlil, and Z. Alabacy, "Industrial picking and packing problem: Logistic management for products expedition," *Journal of Mechanical Engineering Research and Developments*, vol. 43, no. 2, pp. 74–80, 2020.

[22] H. Al-Khazraji, S. Khlil, and Z. Alabacy, "Cuckoo Search Optimization for solving Product Mix Problem," *IOP Conf. Ser. Mater. Sci. Eng.*, vol. 1105, no. 1, p. 012016, 2021.

[23] H. AL-Khazraji, A. Nasser, and S. Khlil, "An intelligent demand forecasting model using a hybrid of metaheuristic optimization and deep learning algorithm for predicting concrete block production," *IAES Int. J. Artif. Intell. (IJ-AI)*, vol. 11, no. 2, p. 649, 2022.

[24] H. Al-Khazraji, "Comparative study of whale optimization algorithm and flower pollination algorithm to solve workers assignment problem," *Int. J. Prod. Manag. Eng*., vol. 10, no. 1, pp. 91–98, 2022.

[25] S. N. Makhadmeh, O. A. Alomari, S. Mirjalili, M. A. Al-Betar, and A. Elnagar, "Recent advances in multi-objective grey wolf optimizer, its versions and applications," *Neural Comput. Appl*., vol. 34, no. 22, pp. 19723–19749, 2022.

[26] A. H. Sule, A. S. Mokhtar, J. J. Bin Jamian, A. Khidrani, and R. M. Larik, "Optimal tuning of proportional integral controller for fixed-speed wind turbine using grey wolf optimizer," *Int. J. Electr. Comput. Eng. (IJECE)*, vol. 10, no. 5, p. 5251, 2020.

[27] T. Dogruer, "Grey wolf optimizer-based optimal controller tuning method for unstable cascade processes with time delay," *Symmetry (Basel)*, vol. 15, no. 1, p. 54, 2022.

[28] S. K. Verma, S. Yadav, and S. K. Nagar, "Optimization of fractional order PID controller using grey wolf optimizer," *J. Control Autom. Electr. Syst*., vol. 28, no. 3, pp. 314–322, 2017.

[29] M. A. Hasan, A. A. Oglah, and M. J. Marie, "Optimal FOPI-FOPD controller design for rotary inverted pendulum system using grey wolves' optimization technique," *TELKOMNIKA (Telecommunication Computing Electronics and Control)*, vol. 21, no. 3, pp. 657–666, 2023.

[30] X. Sun, C. Hu, G. Lei, Y. Guo, and J. Zhu, "State feedback control for a PM hub motor based on gray wolf optimization algorithm," *IEEE Trans. Power Electron*., vol. 35, no. 1, pp. 1136–1146, 2020.

[31] W. M. Jasim, "State feedback based on grey wolf optimizer controller for two-wheeled self-balancing robot," *J. Intell. Syst*., vol. 31, no. 1, pp. 511–519, 2022.

[32] D. Koulocheris, G. Papaioannou, and D. Christodoulou, "Assessment of the optimization procedure for the nonlinear suspension system of a heavy vehicle," *Mobility and Vehicle Mechanics*, vol. 42, no. 2, pp. 17–35, 2016.

[33] D. Zhao, M. Du, T. Ni, M. Gong, and L. Ma, "Dual adaptive robust control for uncertain nonlinear active suspension systems actuated by asymmetric electrohydraulic actuators," *Low Freq. Noise Vibr*., vol. 40, no. 3, pp. 1607–1632, 2021.

[34] A. K. Ahmed and H. Al-Khazraji, "Optimal control design for propeller pendulum systems using gorilla troops optimization," *J. Eur. Syst. Autom*., vol. 56, no. 4, pp. 575–582, 2023.

[35] H. AL-Khazraji, C. Cole, and W. Guo, "Analysing the impact of different classical controller strategies on the dynamics performance of production-inventory systems using state space approach," *J. Model. Manag*., vol. 13, no. 1, pp. 211–235, 2018.

[36] Z. N. Mahmood, H. Al-Khazraji, and S. M. Mahdi, "PID-Based Enhanced Flower Pollination Algorithm Controller for Drilling Process in a Composite Material," *Annales de Chimie Science des Matériaux*, vol. 47, 2023.

[37] A. M. Saeed and K. S. Rijab, "PID controller enhanced A* algorithm for efficient water boat," *J. Eur. Syst. Autom.*, vol. 56, no. 6, pp. 1083–1093, 2023.

[38] L. T. Rasheed, N. Q. Yousif, and S. Al-Wais, "Performance of the optimal nonlinear PID controller for position control of antenna azimuth position system," *Mathematical Modelling of Engineering Problems*, vol. 10, no. 1, 2023.

[39] R. S. Patil, S. P. Jadhav, and M. D. Patil, "Review of Intelligent and Nature-Inspired Algorithms-Based Methods for Tuning PID Controllers in Industrial Applications," *Journal of Robotics and Control (JRC)*, vol. 5, no. 2, pp. 336–358, 2024.

[40] H. Al-Khazraji and L. T. Rasheed, "Performance evaluation of Pole Placement and Linear Quadratic Regulator strategies designed for Mass-Spring-Damper system based on Simulated Annealing and Ant Colony optimization," *J. Eng.*, vol. 27, no. 11, pp. 15–31, 2021.

[41] S. Mirjalili, S. M. Mirjalili, and A. Lewis, "Grey wolf optimizer," *Adv. Eng. Softw.*, vol. 69, pp. 46–61, 2014.

[42] H. A. Hadi, A. Kassem, H. Amoud, S. Nadweh, and N. M. Ghazaly, "Using Grey Wolf Optimization Algorithm and Whale Optimization Algorithm for Optimal Sizing of Grid-Connected Bifacial PV Systems," *Journal of Robotics and Control (JRC)*, vol. 5, no. 3, pp. 733–745, 2024.

[43] M. Zawbaa, C. Grosan, and A. E. Hassenian, "Feature subset selection approach by gray-wolf optimization," in *Advances in Intelligent Systems and Computing*, pp. 1–13, 2015.

[44] J. Agarwal, G. Parmar, R. Gupta, and A. Sikander, "Analysis of grey wolf optimizer based fractional order PID controller in speed control of DC motor," *Microsyst. Technol.*, vol. 24, no. 12, pp. 4997–5006, 2018.

[45] E. V. Kuliev, V. V. Kureichik, and I. O. Kursitys, "Decision making in VLSI components placement problem based on grey wolf optimization," in *2019 IEEE East-West Design & Test Symposium (EWDTS)*, pp. 1-4, 2019.

[46] S. Mohammad Aghdam, F. Soleimanian Gharehchopogh, and M. Masdari, "Opinion Leader's Selection with Grey Wolf Optimizer Algorithm on Social Networks," *International Journal of Industrial Mathematics*, vol. 13, no. 2, pp. 163–174, 2021.

[47] N. M. Hatta, A. M. Zain, R. Sallehuddin, Z. Shayfull, and Y. Yusoff, "Recent studies on optimisation method of Grey Wolf Optimiser (GWO): a review (2014–2017)," *Artif. Intell. Rev.*, vol. 52, no. 4, pp. 2651–2683, 2019.

[48] D. K. Geleta, M. S. Manshahia, P. Vasant, and A. Banik, "Grey wolf optimizer for optimal sizing of hybrid wind and solar renewable energy system," *Comput. Intell.*, vol. 38, no. 3, pp. 1133–1162, 2022.

[49] P. Meiwal, H. Sharma, and N. Sharma, "Fully informed grey wolf optimizer algorithm," in *Information Management and Machine Intelligence: Proceedings of ICIMMI 2019*, pp. 497–512, 2021.

[50] A. Ahmed, R. Gupta, and G. Parmar, "GWO/PID approach for optimal control of DC motor," in *2018 5th International Conference on Signal Processing and Integrated Networks (SPIN)*, 2018.

[51] Y. Hou, H. Gao, Z. Wang, and C. Du, "Improved grey wolf optimization algorithm and application," *Sensors (Basel)*, vol. 22, no. 10, p. 3810, 2022.

[52] S. N. Makhadmeh, O. A. Alomari, S. Mirjalili, M. A. Al-Betar, and A. Elnagar, "Recent advances in multi-objective grey wolf optimizer, its versions and applications," *Neural Comput. Appl.*, vol. 34, no. 22, pp. 19723–19749, 2022.

[53] H. Al-Khazraji, R. M. Naji, and M. K. Khashan, "Optimization of Sliding Mode and Back-Stepping Controllers for AMB Systems Using Gorilla Troops Algorithm," *Journal Européen des Systèmes Automatisés*, vol. 57, no. 2, pp. 417–424, 2024.

[54] A. S. Ahmed and S. K. Kadhim, "A comparative study between convolution and optimal backstepping controller for single arm pneumatic artificial muscles," *Journal of Robotics and Control*, vol. 3, no. 6, pp. 769–778, 2022.

[55] Z. N. Mahmood, H. Al-Khazraji, and S. M. Mahdi, "Adaptive Control and Enhanced Algorithm for Efficient Drilling in Composite Materials," *Journal Européen des Systèmes Automatisés*, vol. 56, no. 3, pp. 507–512, 2023.

[56] N. S. Mahmood, A. J. Humaidi, and R. S. Al-Azzawi, "Extended state observer design for uncertainty estimation in electronic throttle valve system," *International Review of Applied Sciences and Engineering*, vol. 15, no. 1, pp. 107–115, 2024.